Preprints.org

Article

Recognition of Granulocyte-Macrophage Colony-Stimulating Factor by Specific S100 Proteins

Alexey S. Kazakov , Victoria A. Rastrygina , Alisa A. Vologzhannikova , Marina Y. Zemskova , Lolita A. Bobrova , Evgenia I. Deryusheva , Maria E. Permyakova , Andrey S. Sokolov , Ekaterina A. Litus , Marina P. Shevelyova , Vladimir N. Uversky [*] , Eugene A. Permyakov , Sergei E. Permyakov [*]

Article

Recognition of Granulocyte-Macrophage Colony-Stimulating Factor by Specific S100 Proteins

**Alexey S. Kazakov [1,†], Victoria A. Rastrygina [1,†], Alisa A. Vologzhannikova [1],
Marina Y. Zemskova [1,2], Lolita A. Bobrova [1], Evgenia I. Deryusheva [1], Maria E. Permyakova [1],
Andrey S. Sokolov [1], Ekaterina A. Litus [1], Marina P. Shevelyova [1], Vladimir N. Uversky [1,3,*],
Eugene A. Permyakov [1] and Sergei E. Permyakov [1,*]**

[1] Pushchino Scientific Center for Biological Research of the Russian Academy of Sciences, Institute for Biological Instrumentation, Institutskaya str., 7, Pushchino, Moscow Region 142290, Russia; fenixfly@yandex.ru (A.S.K.); certusfides@gmail.com (V.A.R.); lisiks.av@gmail.com (A.A.V.); bobrovalola@gmail.com (L.A.B.); janed1986@ya.ru (E.I.D.); mperm1977@gmail.com (M.E.P.); 212sok@gmail.com (A.S.S.); ealitus@gmail.com (E.A.L.); marina.shevelyova@gmail.com (M.P.S.); epermyak@yandex.ru (E.A.P.)

[2] Pushchino Scientific Center for Biological Research of the Russian Academy of Sciences, G.K. Skryabin Institute of Biochemistry and Physiology of Microorganisms, pr. Nauki, 5, Pushchino, Moscow Region 142290, Russia; marinazemskova9@gmail.com (M.Y.Z.)

[3] Department of Molecular Medicine and USF Health Byrd Alzheimer's Research Institute, Morsani College of Medicine, University of South Florida, Tampa, FL 33612, USA; vuversky@usf.edu (V.N.U.)

* Correspondence: vuversky@usf.edu (V.N.U.); permyakov.s@gmail.com (S.E.P.); Tel.: +7-(495)-143-7740 (S.E.P.); Fax: +7-(4967)-33-05-22 (S.E.P.).

† Equal contributions.

Abstract: Granulocyte-macrophage colony-stimulating factor (GM-CSF) is a pleiotropic myelopoietic growth factor and proinflammatory cytokine, clinically used for multiple indications and serving as a promising target for treatment of many disorders, including cancer, multiple sclerosis, rheumatoid arthritis, psoriasis, asthma, COVID-19. We have previously shown that dimeric Ca^{2+}-bound forms of S100A6 and S100P proteins, members of the multifunctional S100 protein family, are specific to GM-CSF. To probe selectivity of these interactions, the affinity of recombinant human GM-CSF to dimeric Ca^{2+}-loaded forms of 18 recombinant human S100 proteins was studied by surface plasmon resonance spectroscopy. Of them, only S100A4 protein specifically binds to GM-CSF with equilibrium dissociation constant, K_d, values of 0.3-2 μM, as confirmed by intrinsic fluorescence and chemical crosslinking data. Calcium removal prevents S100A4 binding to GM-CSF, whereas monomerization of S100A4/A6/P proteins disrupts S100A4/A6 interaction with GM-CSF and induces a slight decrease in S100P affinity for GM-CSF. Structural modelling indicates the presence in the GM-CSF molecule of a conserved S100A4/A6/P-binding site, consisting of the residues from its termini, helices I and III, some of which are involved in the interaction with GM-CSF receptors. The predicted involvement of the 'hinge' region and F89 residue of S100P in GM-CSF recognition was confirmed by mutagenesis. Examination of S100A4/A6/P ability to affect GM-CSF signaling showed that S100A4/A6 inhibit GM-CSF/S100-induced suppression of viability of monocytic THP-1 cells. The ability of the S100 proteins to modulate GM-CSF activity is relevant to progression of various neoplasms and other diseases, according to bioinformatics analysis. The direct regulation of GM-CSF signaling by extracellular forms of the S100 proteins should be taken into account in the clinical use of GM-CSF and development of the therapeutic interventions targeting GM-CSF or its receptors.

Keywords: GM-CSF; S100A4; S100A6; S100P; protein–protein interaction; cell viability

1. Introduction

Granulocyte-macrophage colony-stimulating factor (GM-CSF; CSF-2) is a pleiotropic 23 kDa short-chain four-helical cytokine (SCOP [1] ID 4000852 and 3001717) belonging along with IL-3 and IL-5 to the β common family of cytokines [2–4]. Basal levels of serum GM-CSF are of 1-4 pM but may rise rapidly in response to infection [5,6]. GM-CSF is normally expressed in lung, urinary bladder, pancreas, bone marrow and some other tissues [7], and is produced at sites of tissue inflammation [5,8]. GM-CSF is produced by T-cells, natural killer cells, alveolar cells type 2, granulocytes, ductal cells, basal respiratory cells, pancreatic endocrine cells, ionocytes, endothelial cells, Langerhans cells [7], other cells under various stimuli, and tumor cells [9,10]. GM-CSF regulates activity of macrophages, including monocytes and microglia, dendritic cells, lymphocytes, granulocytes, endothelial cells, pneumocytes type I, mesenchymal cells, *etc.* [6,11,12]. Thus, GM-CSF modulates activity of the innate immune cells serving as a bridge to the activation of adaptive immunity, thereby globally affecting host immunity under pathological conditions [9].

GM-CSF is a colony-stimulating factor along with M-CSF (CSF-1) and G-CSF (CSF-3), the growth factors that favor formation of myeloid colonies from bone marrow precursors [5,13]. Some other cytokines, such as IL-3, IL-5, and IL-34, are also involved in myelopoiesis [5]. G-CSF and M-CSF/IL-34 signal through the homodimeric receptors G-CSF-R and CSF-1-R, respectively [5]. In contrast, GM-CSF, IL-3, and IL-5 signal via the heterodimeric complex consisting of the cytokine-specific α chain (GM-CSF receptor subunit α, CD116, for GM-CSF) and a shared signal-transducing Cytokine receptor common subunit β (CD131) [5]. Erythropoietin is able to signal in the both manners [14]. CD116 has two isoforms and a truncated, soluble form [11]. The hexameric complex of GM-CSF with its receptors contains two intertwined CD131 chains in the center, surrounded by two CD116 chains with two GM-CSF molecules wrapped by the CD116 and CD131 chains [4,11]. Dimerization of the hexamer brings the cytoplasmic domains of the CD131 chains into proximity, which is thought to be crucial for the subsequent signaling events [4]. The GM-CSF signaling pathways include JAK-STAT5, PI3K-AKT, MEK-ERK, NF-κB, β-catenin/Tcf4, JMJD3/IRF-4, IFN-γ-R/IRF-1, and AKT-mTOR [4,5,8,15–17].

Sulfated glycosaminoglycans, heparan sulfate proteoglycans, including Syndecan-2, are implicated in modulation of GM-CSF signaling [18,19]. The sophisticated signaling system of GM-CSF contributes to its multifactorial impact on host immune responses, and its involvement in pathogenesis of many diseases, including inflammatory arthritis, osteoarthritis, multiple sclerosis, inflammatory bowel disease, asthma, interstitial lung disease, pulmonary alveolar proteinosis, COVID-19, aortic aneurysm, obesity and its associated meta-inflammation, cancers, and other disorders [5,11,15,20,21].

Elevated GM-CSF expression drives production of pro-inflammatory cytokines/chemokines (IL-1, IL-6, TNF, CCL2, IL-8, CCL17, *etc.*), excessive inflammation, chemotaxis, and tissue damage [22]. Therefore, several monoclonal antibodies that neutralize either GM-CSF (Otilimab, Namilumab, Gimsilumab, Plonmarlimab, and Lenzilumab) or CD116 (Mavrilimumab)/CD131 (CSL311) are currently in clinical trials for treatment of multiple sclerosis, rheumatoid arthritis, osteoarthritis, psoriatic arthritis, plaque psoriasis, asthma, COVID-19, lymphoma and leukemia [4,15,23].

Meanwhile, GM-CSF suppresses autoimmune diabetes and autoimmune thyroiditis, systemic lupus erythematosus, myasthenia gravis, inflammatory bowel disease, atherosclerosis, some cancers, *etc.* [8,9,24]. Recombinant human GM-CSF with substitution at L23, known as sargramostim (Leukine®), is clinically used for neutrophil recovery and reduction of the incidence of the infections following induction chemotherapy in older patients with acute myeloid leukemia; mobilization of hematopoietic progenitor cells into peripheral blood for collection by leukapheresis and transplantation; acceleration of myeloid reconstitution following bone marrow or peripheral blood progenitor cell transplantation; treatment of delayed neutrophil recovery or graft failure after bone marrow transplantation; treatment of the patients acutely exposed to myelosuppressive doses of radiation. Another recombinant GM-CSF, molgramostim, has been used in the clinical trials for cystic fibrosis, bronchiectasis, pulmonary alveolar proteinosis, acute respiratory distress syndrome, COVID-19, Mycobacterium and Hepatitis B infections, and several cancers. GM-CSF alone or in

combination with chemotherapy, monoclonal antibodies/cancer vaccines is being tested in clinical trials for numerous cancers [9].

GM-CSF incorporated into vaccines (GM-CSF-secreting cancer cell vaccines, GM-CSF-fused tumor-associated antigen protein-based vaccines, GM-CSF-based DNA vaccines, and GM-CSF-producing oncolytic viruses) stimulates potent antitumor responses, probably by promoting differentiation and activation of dendritic cells [4,9]. The clinically approved GM-CSF-based cancer vaccines include Sipuleucel-T (Provenge®), a cell-based cancer immunotherapy for treatment of prostate cancer, and Talimogene laherparepvec (IMLYGIC®), an oncolytic herpes virus for advanced melanoma treatment. Many investigational GM-CSF-based cancer vaccines are currently in trials: cancer-specific GVAX vaccines, Pexa-Vec®, Vigil®, ONCOS-102, OrienX010, MVX-ONCO-1, and STINGVAX.

Therefore, both inhibition and stimulation of GM-CSF activity are valuable therapeutic options depending on the specific disorder and its stage. The global GM-CSF market is valued at US $1.5 billion in 2021 and is expected to reach US $3.4 billion in 2029 [25], in part due to the presence of the numerous drug candidates undergoing clinical trials. For this reason, knowledge of the factors affecting GM-CSF activity is important for both the development and effective use of the drugs targeting GM-CSF signaling.

Despite the vast knowledge of the mechanisms of GM-CSF signaling and its contribution to cellular homeostasis in both health and disease, the regulation of GM-CSF activity by extracellular soluble proteins remains largely unexplored. We recently showed that the members of the S100 family of Ca^{2+}-binding proteins, S100P and S100A6, specifically interact with GM-CSF and many other four-helical cytokines under physiological *in vitro* conditions [26,27]. The S100 protein family includes over 20 regulatory multifunctional proteins consisting of two Ca^{2+}-binding motifs linked by a flexible 'hinge' region: a canonical C-terminal EF-hand and a low-affinity N-terminal pseudo-EF-hand [28,29]. Ca^{2+} binding typically alters structure of a S100 protein, resulting in changes in its affinity for binding partners such as soluble regulatory proteins, receptor/membrane proteins, nucleic acids and lipids, thereby implicating S100 proteins in multiple physiological processes [30–32]. When S100 proteins are released into the extracellular space, some of them interact with cell surface receptors (RAGE, TLR4, ErbB1, ErbB3, ErbB4, IL-10R, integrin β1, neuroplastin-β, 5-HT1B, 4-HT4, SIRL-1, ALCAM, EMMPRIN, CD33, CD36, CD68, CD69, and CD146 [26]), acting in a cytokine-like manner [29,32,33]. In addition, extracellular forms of certain S100 proteins have been shown to bind specific cytokines, in some cases exerting distinct cellular effects [26,27,34–47]. Such a broad network of S100 interactions seems to contribute to their involvement in the progression of many socially significant diseases (oncological, neurological, inflammatory, autoimmune, cardiovascular and respiratory diseases), and suggests the use of S100 proteins as diagnostic and therapeutic targets [29,32,33,48–51].

In this work, we reveal new aspects of regulation of GM-CSF activity by S100 proteins: we explored selectivity of GM-CSF interaction with S100 proteins, conformational prerequisites for the GM-CSF – S100 interactions, and the cellular effects they exert.

2. Materials and Methods

2.1. Materials

Recombinant tag-free human S100A1/A3/A4/A5/A6/A7/A8/A9/A10/A11/A12/A13/A14/A15/A16/B/P proteins were expressed in *E. coli* and purified as described in [41,42,46,47]. Recombinant tag-free human S100A7L2/G/Z proteins and GM-CSF were produced in *E. coli* as described below. Human S100P mutants F89A and Δ42–47 (lacks PGFLQS sequence in the 'hinge' reion) were prepared according to [47]. The protein concentrations were determined spectrophotometrically according to [52]. Catalytic light chain of bovine enteropeptidase was purchased from New England Biolabs Inc. (Ipswich, MA, USA).

Phosphate, imidazole, HEPES, Tris, sodium chloride, sodium hydroxide, SDS, DTT, glycerol, L-arginine, urea, as well as reduced and oxidized L-glutathione were purchased from PanReac

AppliChem (Barcelona, Spain). IPTG and PMSF were purchased from Helicon (Moscow, Russia). Calcium chloride, EDTA, TWEEN 20 and glutaric aldehyde were from Sigma–Aldrich Co. (Burlington, MA, USA). Silver staining of electrophoresis gels was carried out using PlusOne™ Silver Staining Kit (Protein) (Amersham Biosciences, Inc., Amersham, UK). Molecular mass marker for SDS-PAGE and SnakeSkin™ dialysis tubing (MWCO of 3.5 kDa) were from Thermo Fisher Scientific, Inc. (Waltham, MA, USA). HiPrep™ 26/60 Sephacryl® S-100 HR was from GE HealthCare (Chicago, IL, USA). Bio-Scale Mini Profinity IMAC cartridge was from Bio-Rad Laboratories, Inc. (Hercules, CA, USA). NAP-5 column was bought from Cytiva (Marlborough, MA, USA). All water solutions were prepared using ultrapure water (Millipore Simplicity 185 system).

Human leukemia monocytic cell line THP-1 was from ATCC (Manassas, VA, USA). RPMI 1640 medium, L-glutamine, penicillin and streptomycin were purchased from PanEco Ltd. (Moscow, Russia). Fetal bovine serum was from Biosera (Cholet, France). MTT was bought from Dia-M (Moscow, Russia). Bovine pancreatic ribonuclease was from Thermo Fisher Scientific Inc. (Waltham, MA, USA). ELISA kit for LPS was from Cloud-Clone Corp. (Wuhan, China).

2.2. Preparation of GM-CSF

The nucleotide sequence (NCBI reference sequence: NM_000758.4) encoding human GM-CSF chain 18-144 (UniProt ID P04141 lacking a signal peptide) was cloned into pET-32mod vector (uses E. coli thioredoxin as a fusion partner; the fusion protein is cleaved by bovine enteropeptidase [53]) between NdeI and XhoI restriction sites. E. coli BL21 (DE3) cells carrying pLacIRARE plasmid were transformed with the resulting plasmid and grown in 2 L of 2xYT medium with 100 µg/mL ampicillin at 30 °C, shaking at 180 rpm, until optical density at 600 nm reached 1 AU. Expression of the thioredoxin–GM-CSF chimera was triggered by 1 mM IPTG. The cells were grown for 5 h, harvested by centrifugation at 5000× g for 15 min at 4 °C, resuspended in 50 mL of 50 mM phosphate, 20% glycerol, 1 mM PMSF, 1 M NaCl, 0.5% TWEEN 20, pH 8.0 buffer, and disintegrated by a French press. The lysate was centrifuged at 30,000× g for 30 min at 4 °C. The pellet containing inclusion bodies of the thioredoxin–GM-CSF chimera was dissolved in 20 mM Tris-HCl, 200 mM NaCl, 1 mM EDTA, 0.5% TWEEN 20, pH 7.0 buffer; the solution was stirred evenly for 15 min, followed by centrifugation at 6,900× g for 15 min at 4 °C. The last steps were repeated again. The pellet was solubilized in 10 mL of 8 M urea solution in 50 mM Tris-HCl, 10 mM DTT, pH 8.0 buffer. The solution was stirred evenly for 2 h at 4 °C, followed by centrifugation at 6,900× g for 15 min at 4 °C. The supernatant was diluted with 50 mM Tris-HCl, 2.7 M urea, pH 8.0 buffer (#1) to reach urea concentration of 5.3 M, followed by dialysis (MWCO of 3.5 kDa) against buffer #1 for 2 h and second dialysis against 50 mM Tris-HCl, 1 M urea, 0.4 M L-arginine, 3 mM reduced L-glutathione, 0.9 mM oxidized L-glutathione, pH 8.0 buffer (#2) overnight at 4 °C. Next day, the solution was dialyzed for 2 h against buffer #2 diluted with distilled water by 50%, then dialyzed against 1 L of 50 mM Tris-HCl, 250 mM NaCl, 0.1 M L-arginine, 3 mM reduced L-glutathione, 0.9 mM oxidized L-glutathione, pH 8.0 buffer for 2 h at 4 °C.

The insoluble material was removed by centrifugation (6,900× g for 15 min at 4 °C) and the supernatant was dialyzed twice against 2 L of distilled water for 2 h at 4 °C. The final dialysis was performed against 1 L of 50 mM phosphate, 150 mM NaCl, pH 8.0 buffer overnight at 4 °C. 20% glycerol, 1 M urea and 0.5% TWEEN 20 were added to the resulting solution, followed by stirring for 30 min and centrifugation at 6,900× g for 15 min at room temperature. The supernatant was loaded onto a Bio-Scale Mini Profinity IMAC Ni-charged column equilibrated with 50 mM phosphate, 1 M NaCl, 20% glycerol, 0.5% TWEEN 20, pH 8.0 buffer (A). The column was washed with an excess of buffer A. The protein was eluted with 50 mM phosphate, 500 mM imidazole, pH 8.0 buffer. The fractions containing thioredoxin–GM-CSF chimera were collected and dialyzed against 20 mM Tris-HCl, 50 mM NaCl, 5% glycerol, pH 8.0 buffer (B) overnight at 4 °C. 2 mM $CaCl_2$ was added to the resulting solution. The thioredoxin–GM-CSF chimera was cleaved by incubation with light chain of bovine enteropeptidase (the eznyme to chimera molar ratio of $1:1.9\times10^6$) for 24 h at room temperature with stirring, centrifugation (6,900× g for 15 min at 4 °C) and one more digestion at the same conditions.
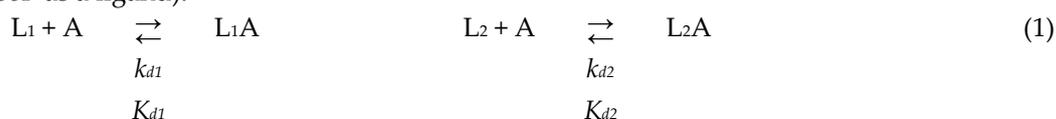
The His-tagged thioredoxin was removed from the sample via passage through the Bio-Scale Mini Profinity IMAC column. The GM-CSF sample was further purified using HiPrep™ 26/60 Sephacryl® S-100 HR gel filtration column equilibrated with 20 mM Tris-HCl, 150 mM NaCl, pH 8.0 buffer (flow rate of 1 mL/min). The fractions corresponding to GM-CSF were collected, concentrated to a concentration of 1.5 mg/mL and stored at −70 °C. The mass of the GM-CSF sample corresponds to residues 18-144 of UniProt ID P04141, which was confirmed by electrospray ionization mass spectrometry according to *[54]*. Functional activity of the GM-CSF sample was verified using an MTT assay as described below.

2.3. Exression and Purification of S100A7L2/G/Z Proteins

The nucleotide sequences encoding human S100A7L2, S100G, S100Z proteins (Uniprot entries Q5SY68, P29377, Q8WXG8, respectively) were codon optimized for expression in E. coli. The syntesized S100 genes were cloned into pHUE vector [55] between the SacII and NotI restriction sites. The ubiquitin-S100 chimera was produced in E. coli BL21 (DE3) cells carrying pLacIRARE plasmid, purified and cleaved by ubiquitin specific peptidase 2, followed by purification of the tag-free S100 protein according to [42] with the following modifications. The cleavage was performed in 20 mM Tris-HCl, 1 mM DTT, pH 8.2 buffer. The subsequent dialysis step was skipped. Purification of S100Z protein using the anion exchange column was carried out at a pH value of 9.7. The final purification of the S100 proteins using the gel filtration column was performed in 10 mM phosphate, 150 mM NaCl, 1 mM 2-ME, pH 7.5 buffer. The purified S100 proteins were stored in 1:1 (v/v) mixture of PBS-glycerol with 1 mM 2-ME at −20 °C.

2.4. Surface Plasmon Resonance Studies

SPR measurements of GM-CSF interaction with S100 proteins at 25 °C were carried out using ProteOn™ XPR36 system (Bio-Rad Laboratories, Inc., Hercules, CA, USA) and amine coupling of a ligand (GM-CSF or S100 protein) to ProteOn GLH sensor chip mainly as described in [27]. When using S100 proteins as a ligand, the surface of the sensor chip was flushed with 0.5% SDS solution to ensure dissociation of the S100 dimer. The running buffer was 10 mM HEPES, 150 mM NaCl, 0.05% TWEEN 20, 1 mM $CaCl_2$ or 5 mM EDTA, pH 7.4. The ligand was regenerated by passage of 20 mM EDTA pH 8.0 solution for 200 s. The double-referenced SPR sensograms were described within a heterogeneous ligand model (1) (GM-CSF serves as a ligand, L; A - analyte) or one-site binding model (S100P as a ligand).

$$L_1 + A \quad \rightleftarrows \quad L_1A \qquad\qquad L_2 + A \quad \rightleftarrows \quad L_2A \qquad\qquad\qquad (1)$$
$$ k_{d1} k_{d2}$$
$$ K_{d1} K_{d2}$$

The corresponding kinetic and equilibrium dissociation constants, k_d and K_d, respectively, were evaluated using Bio-Rad ProteOn Manager™ v.3.1 software (Bio-Rad Laboratories, Inc.). The k_d/K_d values were estimated for 5 analyte concentrations, followed by their averaging (standard deviations are indicated).

2.5. Fluorimetric Studies

Fluorescence measurements were performed using a Cary Eclipse spectrofluorometer (Varian, Inc., Palo Alto, CA, USA) mainly according to [43]. 0.57 μM GM-CSF solution in 10 mM HEPES-NaOH, 150 mM NaCl, 1 mM $CaCl_2$, pH 7.4 buffer was titrated at 25 °C by stock solution of S100A4 in the same buffer. Tryptophan fluorescence of GM-CSF was excited at 295 nm (S100A4 lacks Trp residues). Excitation and emission monochromator bandwidths were 5 nm and 10 nm, respectively. The fluorescence spectra were smoothed by a log-normal function [56] using LogNormal software (IBI RAS, Pushchino, Russia). The dependence of fluorescence emission intensity at 360 nm on S100A4 to GM-CSF molar ratio was described by a one-site binding model using FluoTitr v.1.42 software (IBI RAS, Pushchino, Russia).

2.6. Chemical Crosslinking

6.7 mg/mL S100A4 in 20 mM Tris-HCl, 10 mM DTT, 20 mM EDTA, pH 8.0 buffer was loaded onto a NAP-5 desalting column and eluted with 10 mM HEPES, 150 mM NaCl, pH 7.4 buffer (A) for calcium removal. 4 μM GM-CSF, S100A4, and their mixtures in various molar ratios were treated with 0.02% glutaric aldehyde at 25 °C for 17 h (buffer A with/without 1 mM $CaCl_2$ for Ca^{2+}-loaded/depleted S100A4, respectively). The reaction was quenched by addition of SDS-PAGE sample loading buffer, followed by SDS-PAGE (15%) with silver staining and gel scanning using Molecular Imager PharosFX Plus System (Bio-Rad Laboratories, Inc., Hercules, CA, USA).

2.7. Structural Modeling of the GM-CSF -– S100A4 Complex

The models of tertiary structure of the complex between GM-CSF and S100A4 were built using ClusPro docking server [57] (accessed on September 15, 2023), based on the crystal structures of human GM-CSF (PDB [58] entry 1CSG, chain A) and Ca^{2+}-bound human S100A4 dimer (PDB ID 2Q91, chains A, B). Selection of the contact residues and the best model for visualization was carried out according to [27,41]. The structural models were drawn using the PyMOL v.2.5.0 software [59] (accessed on September 15, 2023).

2.8. Cell Viability Studies

GM-CSF and S100A4/A6/P samples were controlled for undetectable LPS levels (protein concentration of 20,000 ng/mL), using the ELISA kit for LPS according to the manufacturer's instructions.

THP-1 cells were cultured at 37 °C in a humidified 5% CO_2 atmosphere in RPMI 1640 medium supplemented with 10% heat-inactivated fetal bovine serum, 2 mM L-glutamine, 100 U/mL penicillin and 100 μg/mL streptomycin. 500 μL of the cell suspension ($4×10^5$ cells per mL) in the serum-free media were treated with 20 ng/mL GM-CSF or 20/100/500/700/1,000/2,000 ng/mL of S100A4/A6/P or their mixture, and incubated at 37 °C in 5% CO_2 atmosphere for 30 min. Then, 50 μL of the cell suspension ($2×10^4$ cells per well) was seeded in quadruplicate in 96-well plates, and 50 μL of the growth medium supplemented with 10% fetal bovine serum was added, followed by cultivation for the next 48 h. After that 10 μL of 5 mg/mL MTT stock solution was added to the cells, and the plates were kept under the same conditions for 3 h. 250 μL of DMSO per well was then added to dissolve the formazan crystals. The absorbance at 590 nm was measured using a FilterMax F5 microplate reader (Thermo Fisher Scientific Inc., Waltham, MA, USA). The experiments were repeated at least four times and the result were averaged.

2.9. Search of the Diseases Associated with GM-CSF and S100A4/A6/P Proteins

The data on the diseases associated with human GM-CSF (UniProt ID P04141), S100A4 (UniProt ID P26447), S100A6 (UniProt ID P06703), S100P (UniProt ID P25815) were collected from the human disease databases DisGeNET v.7.0 [60] (accessed on September 5, 2023) and Open Targets Platform v.20.09 [61] (accessed on September 6, 2023) as described in [43]. The DisGeNET entries were manually curated; false positive records were removed.

3. Results and Discussion

3.1. GM-CSF Binding to S100 Proteins

SPR spectroscopy screening of specificity of Ca^{2+}-loaded (1 mM $CaCl_2$) forms of 18 recombinant human S100 proteins, S100A1/A3/A4/A5/A7/A7L2/A8/A9/A10/A11/A12/ A13/A14/A15/A16/B/G/Z, to recombinant human GM-CSF immobilized on the surface of SPR sensor chip by amine coupling showed that only S100A4 exhibited noticeable SPR signals at S100 protein concentration of 1 μM. The SPR sensograms for 0.5-8 μM S100A4 were described by the heterogeneous ligand model (1) (Figure 1A), previously used in studies of S100 interactions with four-helical cytokines [26,27,41–47]. The equilibrium dissociation constants, K_d, estimated for S100A4 protein, 0.5 μM and 2.4 μM, resemble

those reported for GM-CSF interaction with S100A6 [26] and S100P [27] (Table 1), and the K_d values for S100A4 complex with GST-RAGE fusion protein (0.6 μM and 1.7 μM [62]). Furthermore, the lowest K_d value for the S100A4 – GM-CSF complex is close to the level of serum S100A4 observed in some pathological conditions (0.1 μM [63]), indicating the potential physiological significance of this complex. In addition, local concentrations of extracellular S100A4 upon injury to S100A4-positive cells may be even higher, favoring formation of S100A4 – GM-CSF complex.

The GM-CSF – S100A4 interaction is strictly Ca^{2+}-dependent, since Ca^{2+} removal by addition of 5 mM EDTA abolishes the S100A4-induced SPR effects (Figure 1A). The calcium sensitivity of target binding to S100A4 protein is explained by the large-scale structural rearrangements in response to Ca^{2+} binding, affecting predominantly helices α2 and α3, the 'hinge' between them, and the both EF-loops of S100A4 [64,65].

As was shown earlier [42], the K_d value for dissociation of Ca^{2+}-loaded S100A4 dimer does not exceed 0.5 μM. Therefore, the SPR estimate of S100A4 affinity for GM-CSF obtained at S100A4 concentrations of 0.5 μM and higher (Table 1) corresponds to S100A4 dimer. To elucidate specificity of GM-CSF to monomeric states of Ca^{2+}-loaded S100A4 and S100A6/P proteins, they were immobilized on the surface of SPR sensor chip by amine coupling, followed by dissociation of the S100 dimers using 0.5% SDS solution. The SPR data for 1 μM GM-CSF revealed notable effects only for S100P protein (Table 1). In this case, the SPR sensograms for 1-8 μM GM-CSF were described by a one-site binding model (Figure 1B). The respective K_d value of 0.8 μM is 2-3 times higher than the previous SPR estimates for GM-CSF binding to Ca^{2+}-bound S100P dimer [27] (Table 1). Notably, this behavior is drastically different from that reported for S100P interaction with the four-helical cytokines IL-11 and IFN-β: S100P monomerization increases its affinity for these cytokines by 1.4 to 2.2 orders of magnitude [43,47,66].
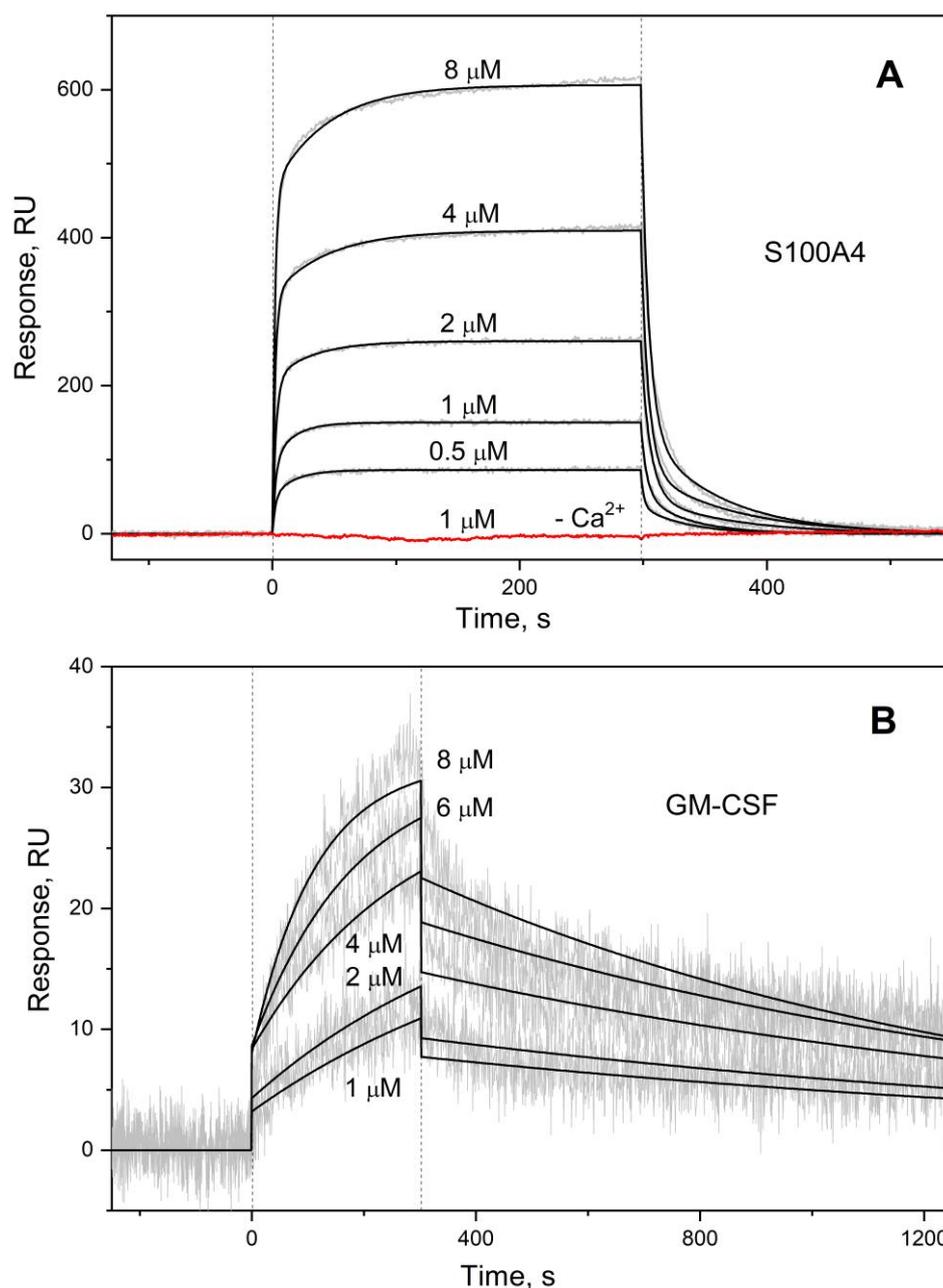
Figure 1. SPR spectroscopy data on kinetics of association/dissociation of the complexes of S100A4 with GM-CSF immobilized on the sensor surface by amine coupling (panel **A**), and GM-CSF with S100P monomer immobilized on the sensor surface (**B**) under calcium excess (1 mM CaCl₂) at 25°C. The sensogram corresponding to calcium-free conditions (5 mM EDTA) is shown in *red*. The association phase is marked by the vertical dotted lines. Analyte concentration is indicated for each sensogram. The experimental curves (*grey*) are described by the heterogeneous ligand model (1) (**A**) or one-site binding model (**B**) (*black*; see Table 1).

Table 1. Parameters of the heterogeneous ligand model (1), describing the SPR data (ligand immobilization on the sensor surface by amine coupling) on kinetics of GM-CSF interaction with the Ca²⁺-loaded S100 proteins at 25 °C.

Analyte	*Ligand*	k_{d1}, s^{-1}	K_{d1}, M	k_{d2}, s^{-1}	K_{d2}, M
S100A4	GM-CSF	$(2.03 \pm 0.70) \times 10^{-2}$	$(4.71 \pm 2.83) \times 10^{-7}$	$(1.65 \pm 0.32) \times 10^{-1}$	$(2.43 \pm 1.22) \times 10^{-6}$
S100A6		$(7.92 \pm 4.02) \times 10^{-4}$ #	$(2.26 \pm 1.18) \times 10^{-6}$ #	$(1.76 \pm 0.49) \times 10^{-2}$ #	$(3.63 \pm 1.14) \times 10^{-6}$ #

S100P		$(1.13 \pm 0.23) \times 10^{-3}$ †	$(2.45 \pm 1.45) \times 10^{-7}$ †	$(6.72 \pm 2.13) \times 10^{-2}$ †	$(4.50 \pm 1.75) \times 10^{-7}$ †
S100P F89A		$(2.83 \pm 1.25) \times 10^{-3}$	$(1.43 \pm 1.03) \times 10^{-6}$	$(4.10 \pm 0.39) \times 10^{-2}$	$(2.02 \pm 0.95) \times 10^{-6}$
GM-CSF	S100A4	n.d.			
	S100A6				
	S100P	$(6.87 \pm 0.71) \times 10^{-4}$ **	$(8.11 \pm 2.14) \times 10^{-7}$ **	-	

ref. [26]; † ref. [27]; n.d., not detected; ** one-site binding model.

SPR measurements require immobilization of the ligand on the surface of the sensor chip, which can shield the analyte-binding site of the ligand from interaction. In order to study the GM-CSF – S100A4 interaction under genuine water solution conditions, we used intrinsic fluorescence spectroscopy and chemical crosslinking with glutaraldehyde (Figure 2). The binding of S100A4 to GM-CSF was monitored by tryptophan fluorescence of the latter in the course of its titration with a stock solution of S100A4 (S100A4 lacks Trp residues). The fluorescence emission intensity at 312 nm shows two distinct processes: S100A4-induced decrease in the intensity with a bend near 1:1 S100A4 to GM-CSF molar ratio, followed by an increase in the fluorescence intensity at higher S100A4 concentrations (Figure 2A). The fluorescence intensity at 360 nm is virtually insensitive to the second process and is adequately described by a one-site binding model with a K_d value of 0.3 μM (Figure 2A), in accord with the SPR estimate (Table 1).

The crosslinking of GM-CSF (4 μM) and Ca^{2+}-loaded/decalcified S100A4 (8 μM) with glutaric aldehyde at 25 °C, followed by SDS-PAGE with silver staining reveals that GM-CSF is fully monomeric, Ca^{2+}-depleted S100A4 is mainly dimeric, whereas Ca^{2+}-bound S100A4 shows presence of dimeric, tetrameric and higher order structures (Figure 2B). The crosslinking data for mixtures of GM-CSF and S100A4 are non-additive, which evidences their complexation. For instance, an additional band appears between 30 and 42 kDa, consistent with the formation of a complex between a GM-CSF molecule and S100A4 dimer (expected mass of 38 kDa), regardless of calcium content. In addition, in the case of Ca^{2+}-depleted S100A4, a marked band appears between 42 and 100 kDa. Meanwhile, in the mixture of GM-CSF with Ca^{2+}-loaded S100A4, accumulation of the higher order structures is observed, and the band corresponding to S100A4 tetramer becomes less pronounced. The decrease in the S100A4 concentration is accompanied by a gradual restoration of the band of GM-CSF monomer. Notably, the observed signs of GM-CSF binding to the decalcified S100A4 are likely related to its partial loading by calcium ions in the solution. Overall, the chemical crosslinking data confirm formation of GM-CSF – S100A4 complexes under genuine water solution conditions, with the K_d values reaching a micromolar level, in agreement with the SPR and fluorescent titration data (Table 1).
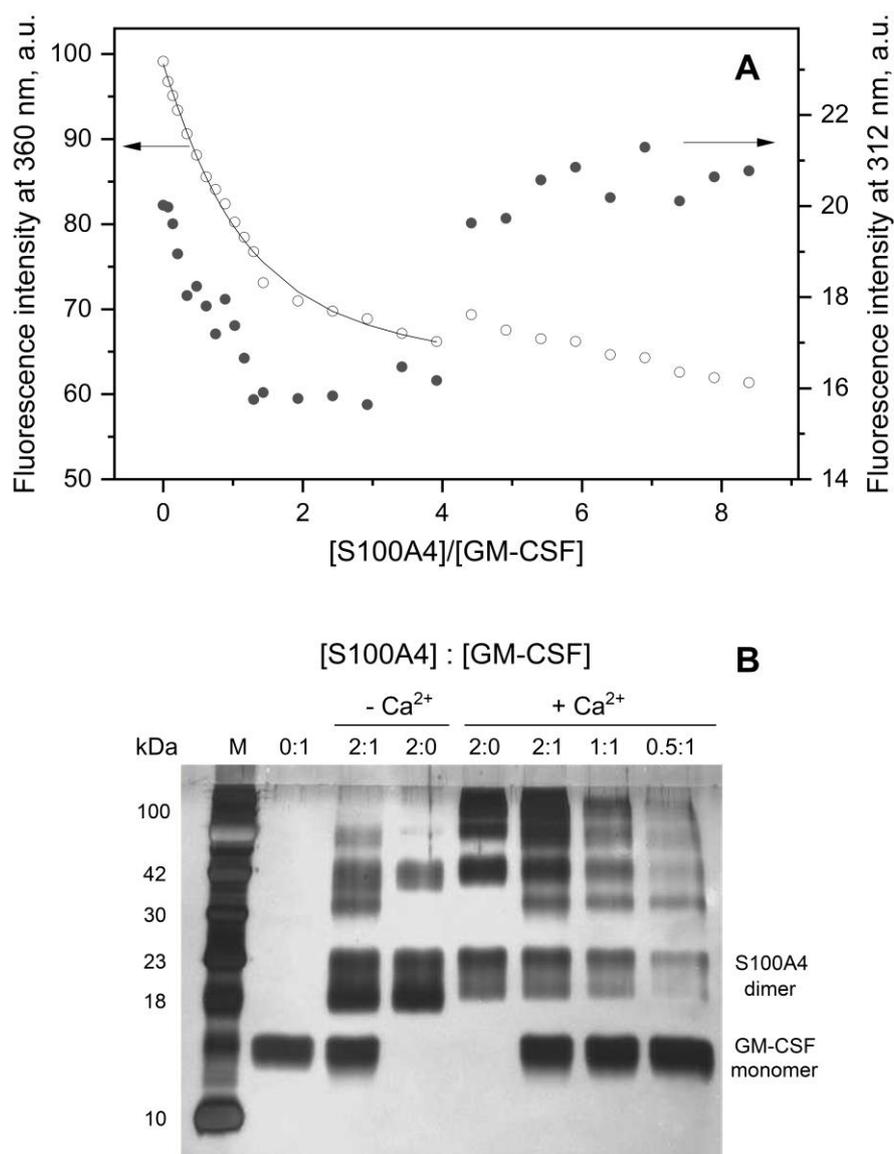
Figure 2. (**A**) Fluorimetric titration of 0.57 μM GM-CSF by Ca^{2+}-loaded S100A4 (1 mM CaC_2) at 25 °C, monitored by tryptophan fluorescence of GM-CSF. The normalized fluorescence intensity at 360 nm is described by a one-site binding model (solid curve). (**B**) The results of SDS-PAGE for GM-CSF (4 μM), Ca^{2+}-depleted/loaded S100A4 and their mixtures crosslinked with glutaric aldehyde at 25 °C (silver staining).

Taken together, these data showed *in vitro* a novel conformation-dependent interaction of GM-CSF with another promiscuous S100 protein [67,68], S100A4. This interaction is non-redundant, since the pairwise sequence identities between S100A4 and S100A6/S100P, which were previously shown to bind GM-CSF [26,27], are 51% and 41%, respectively, according to Clustal Omega v.1.2.4 (EMBL-EBI service [69], accessed on October 15, 2023). Examination of IntAct [70] and BioGRID [71] databases (accessed on October 15, 2023) revealed only two known non-S100 soluble non-receptor extracellular binding partners of GM-CSF: Alpha-2-macroglobulin (UniProt ID: P01023) and Heterogeneous nuclear ribonucleoproteins A2/B1 (UniProt ID: P22626).

3.2. Structural Modeling of the GM-CSF – S100A4 Complex

The modeling of tertiary structure of the GM-CSF complex with Ca^{2+}-loaded S100A4 dimer using ClusPro docking server [57] predicts (Figure 3) that the S100A4-binding site of GM-CSF consists of the residues from the N-terminus (S5, P6, T10 and Q11), helix I (W13, E14, V16, N17, Q20, E21, R23,

R24), helix III (K72, M79) and C-terminus (L115, V116, I117, F119, D120). The predicted S100A4-binding site of GM-CSF is remarkably similar to the previously predicted S100A6/P-binding sites [26,27] (Figure 3A-D).

The same analysis predicts that chain A of S100A4 protein binds GM-CSF by the residues from the helix III (residues K57, N61), EF-loop 2 (R66) and helix IV (Q73), whereas chain B of S100A4 interacts with GM-CSF via residues of the helix II (F45), EF-loop 1 (R49), helix III (K57, N61), EF-loop 2 (S64, R66) and helix IV (Q73, V77, C81 and M85) (Figure 3E). Notably, the predicted S100A4/A6/P-binding sites of GM-CSF differ substantially from each other (Figure 3A-C,E). However, the S100 regions commonly predicted to recognize GM-CSF are helix IV (especially its C-terminal half), helix III (S100A4/A6), and the 'hinge' region (S100A4/P). To verify these predictions, we examined by SPR spectroscopy GM-CSF affinity for the Ca^{2+}-bound S100P mutants F89A (helix IV) and Δ42–47 (lacks PGFLQS sequence in the 'hinge') (Figure S1), which have previously been shown to retain stability of their secondary, tertiary and quaternary structures [27]. The lowest K_d value for the F89A mutant is 6 times higher compared to that for the wild-type protein (Table 1), while Δ42–47 did not reveal specificity to GM-CSF (the K_d values exceed 10^{-4} M), in accord with the modelling results. Similar results were previously obtained for the binding of S100P to many other four-helical cytokines [27].

Several residues of the predicted S100A4/A6/P-binding sites of GM-CSF were previously shown to bind to its receptors (Figure 3D): residues N17, Q20, E21 and R24 bind Cytokine receptor common subunit β (PDB ID 4NKQ), while L115, I117 and F119 interact with GM-CSF receptor subunit α (PDB ID 4RS1). Therefore, S100A4/A6/P binding to GM-CSF is expected to interfere with its association with the receptors. Similarly, some residues of the predicted GM-CSF-binding sites of S100A6/P [26,27] are known to bind V domain of RAGE: K89 of S100A6 (PDB entry 2M1K), and the residues M1, T2, E5, G9, D13, R17, P42, G43, F44, Y88 and F89 of S100P (PDB entry 2MJW). Hence, GM-SCF binding should prevent S100A6/P interaction with RAGE.
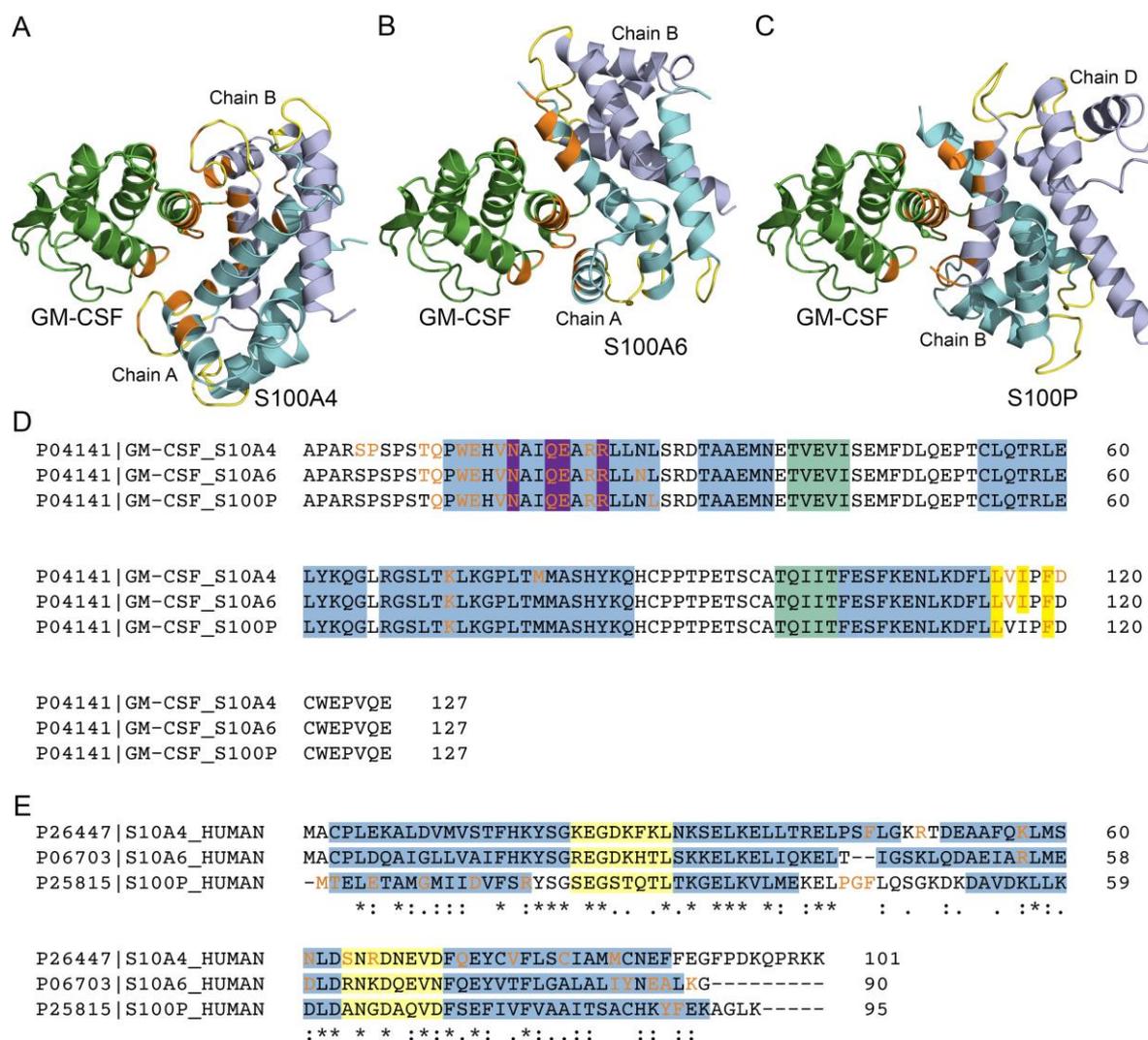
Figure 3. Panels **A-C**: the models of tertiary structures of GM-CSF (*green*) complexes with Ca^{2+}-bound S100A4/A6/P dimers predicted using ClusPro docking server [57]. The data for S100A6/P proteins are taken from [26,27]. The contact residues and the Ca^{2+}-binding loops are shown in orange and yellow, repetively. (**D**) Mapping of the predicted contact residues of GM-CSF (*orange*) in complex with S100A4/A6/P dimers onto its amino acid sequence. The α-helices and β-sheets are marked according to the PDB entry in dark *blue* and *green*, respectively. The residues highlighted in *yellow* and *purple* are involved in recognition of GM-CSF receptor subunit α (PDB ID 4RS1) and Cytokine receptor common subunit β (PDB ID 4NKQ), respectively. (**E**) Mapping of the predicted contact residues of S100A4/A6/P dimers (*orange*) in complex with GM-CSF onto their aligned amino acid sequence (Clustal Omega v.1.2.4, EMBL-EBI service [12] accessed on October 20, 2023). The α-helices and Ca^{2+}-binding loops are marked according to the PDB entries in dark *blue* and *yellow*, respectively.

3.3. Impact of GM-CSF, S100 Proteins and Their Mixtures on Viability of THP-1 Cells

To probe the ability of the interaction between GM-CSF and S100A4/A6/P to affect functional activities of the both interaction partners, we studied the influence of extracellualar GM-CSF, S100A4/A6/P proteins, and their mixtures on viability of human leukemia monocytic cell line THP-1 using an MTT assay (Figures 4–6). THP-1 serves as a common model for functional studies of monocytes and macrophages [72] and is known to be sensitive to GM-CSF: treatment of THP-1 cells with 20 ng/mL GM-CSF leads to JAK2/STAT5 phosphorylation [73]. Since possible contamination of the recombinant protein samples with LPS may alter activities of THP-1 cells [74], GM-CSF and S100A4/A6/P samples were examined for LPS content using an ELISA kit for LPS. All protein samples

were negative for LPS at a protein concentration of 20,000 ng/mL, an order of magnitude higher than the maximum concentration used in the MTT assays.

Incubation of THP-1 cells with 20 ng/mL (1.4 nM) GM-CSF alone decreased cell viability by 18–23% (Figures 4B, 5B and 6B). The similar inhibitory effect of 17–26% was observed in the cells treated with 20-2,000 ng/mL (2-172/196 nM) S100A4/A6 proteins (Figures 4A and 5A). Meanwhile, co-administration of GM-CSF and S100A4 or S100A6 at the same concentrations remarkably rescued THP-1 cells from the GM-CSF-induced cytotoxicity (Figures 4B and 5B). Moreover, in the case of S100A4, this effect gradually developed with increasing S100A4 concentration, leading to the nearly complete recovery of cell viability to the level of the control (Figure 4B). The non-additive effect of simulataneous application of extracellular GM-CSF and S100A4/A6 may indicate formation of their complex, which has a drastically different activity towards THP-1 cells. The inhibitory action of this complex is consistent with the structural modeling results described above. The analogous effect on viability of MCF-7 breast cancer cells was previously described for the S100A1/A4/B/P binding to another four-helical cytokine, IFN-β [42–44].

The addition of 20-2,000 ng/mL (1.9-192 nM) S100P to THP-1 cells was accompanied by suppression of their viability by 12-22% (Figure 6A). The combined application of 20 ng/mL (1.4 nM) GM-CSF and S100P at the same concentrations reduced cell viability by 33-48% (Figure 6B). Thus, the cellular effects exerted by GM-CSF and S100P are nearly additive, which may evidence that their interaction does not affect functional activities of the interaction partners, or that GM-CSF does not bind S100P under these conditions.
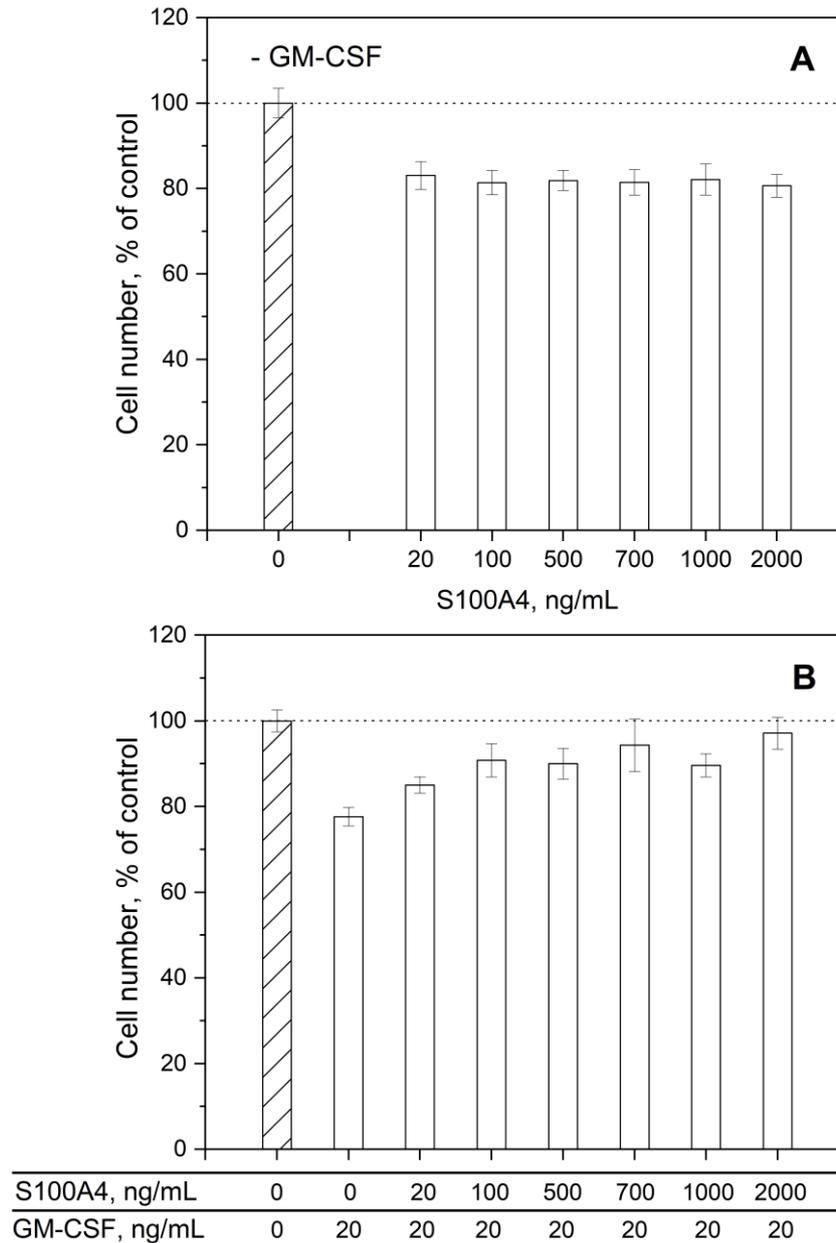
Figure 4. The changes in viability of THP-1 cells in response to extracellular S100A4 protein (20-2,000 ng/mL; 1.7-172 nM) (panel **A**), GM-CSF (20 ng/mL; 1.4 nM) or their combination (**B**), according to an MTT assay. The standard deviations are indicated.
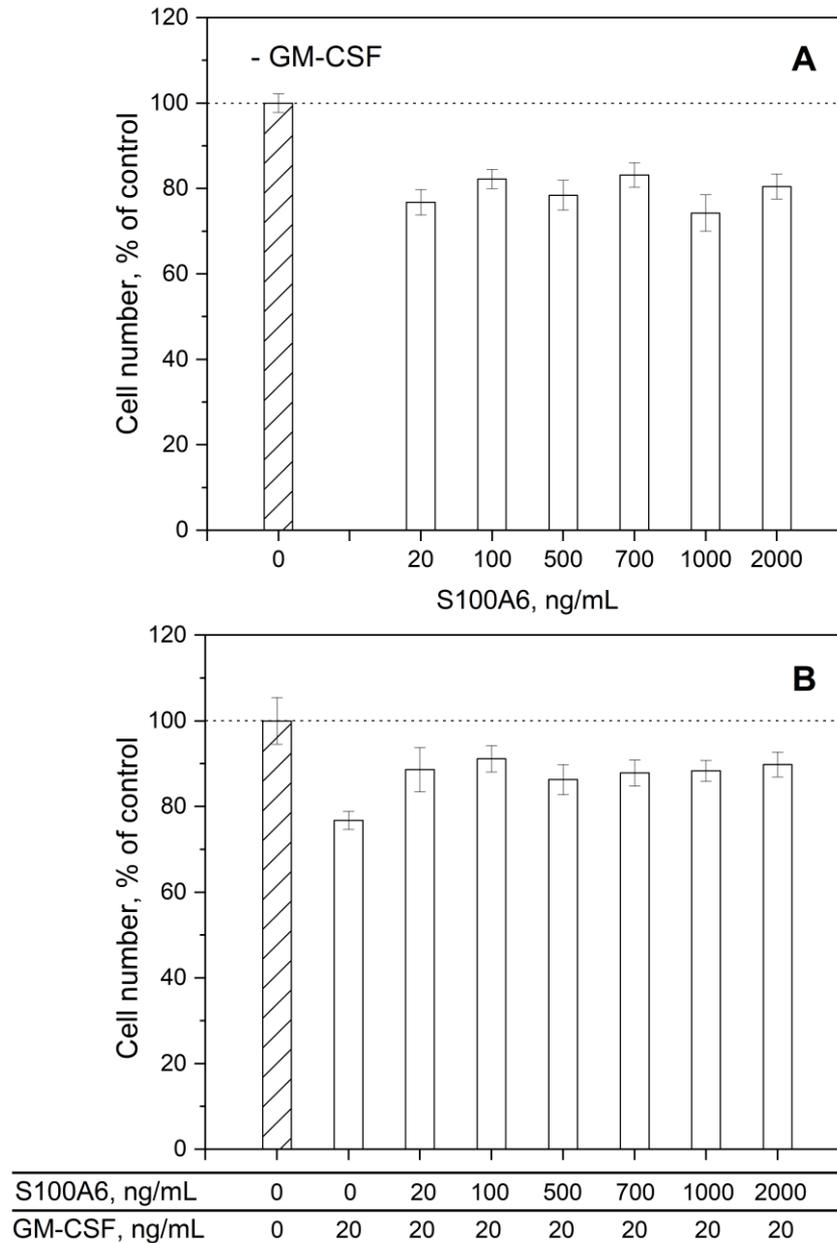
Figure 5. The changes in viability of THP-1 cells in response to extracellular S100A6 protein (20-2,000 ng/mL; 2.0-196 nM) (panel **A**), GM-CSF (20 ng/mL; 1.4 nM) or their combination (**B**), according to an MTT assay. The standard deviations are indicated.
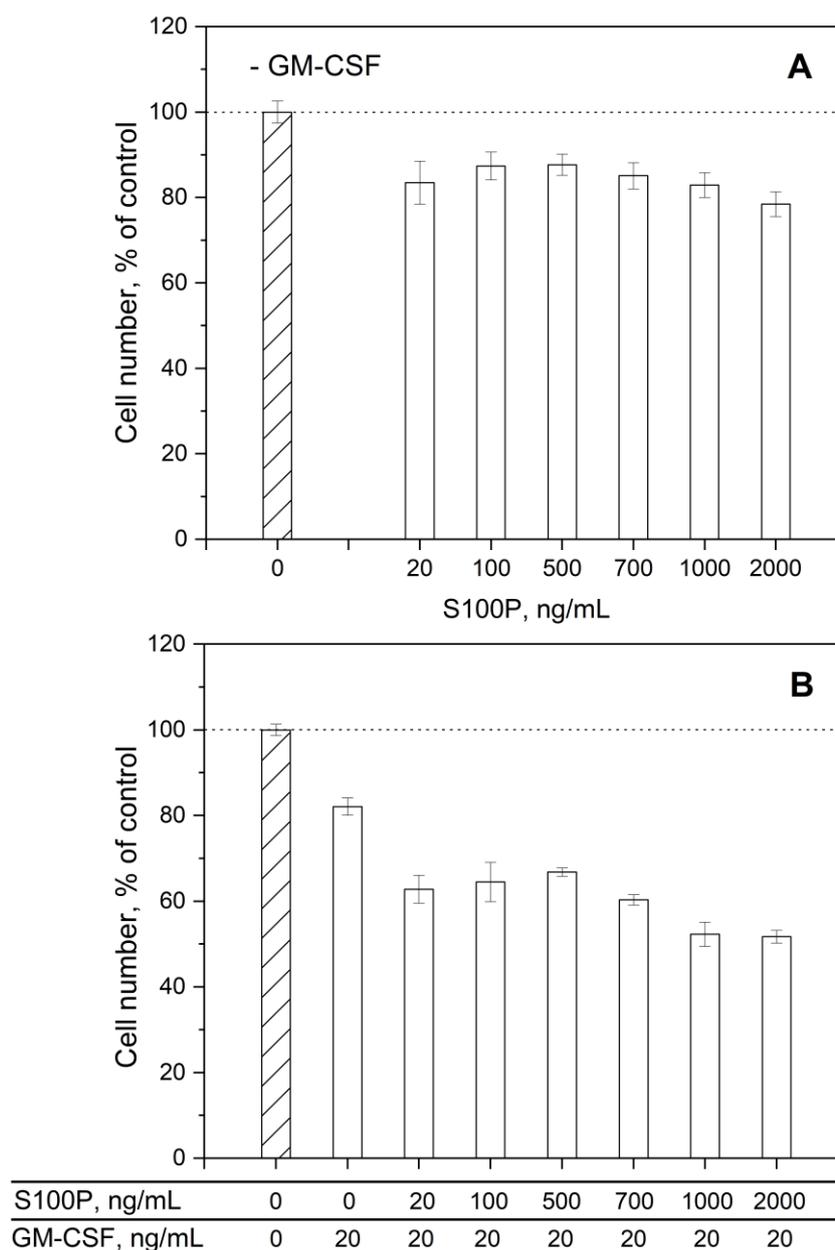
Figure 6. The changes in viability of THP-1 cells in response to extracellular S100P protein (20-2,000 ng/mL; 1.9-192 nM) (panel **A**), GM-CSF (20 ng/mL; 1.4 nM) or their combination (**B**), according to an MTT assay. The standard deviations are indicated.

3.4. Human Diseases Associated with Dysregulation of GM-CSF and S100A4/A6/P Proteins

To elucidate the possible involvement of the GM-CSF – S100A4/A6/P interactions in pathogenesis of diseases, we searched the DisGeNET [60] and Open Targets Platform ('OTP') [61] databases for the human diseases associated with simultaneous involvement of the both interaction partners.

DisGeNET contains 127 entries related to both GM-CSF and S100A4, most of which are various neoplasms (Table S1). OTP database includes 291 entries associated with both GM-CSF and S100A4 (Table S2); the entries with the association scores exceeding 0.1 are 'cancer', 'genetic disorder', 'hepatocellular carcinoma', and 'neoplasm'.

DisGeNET includes 67 entries related to both GM-CSF and S100A6: different neoplasms, Alzheimer's disease, and others (Table S3). OTP database contains 276 entries associated with both

GM-CSF and S100A6 (Table S4). Consideration of the entries with association scores above 0.1 reveals 'genetic disorder' and 'neoplasm'.

DisGeNET contains 4 entries related to both GM-CSF and S100P: various neoplasms and osteoporosis (Table S5). OTP database includes 155 entries associated with both GM-CSF and S100P (Table S6); the entries with the association scores exceeding 0.1 are 'genetic disorder' and 'neoplasm'.

Examination of the DisGeNET database revealed no diseases co-associated with GM-CSF, S100A4, S100A6 and S100P. Meanwhile, OTP database contains 84 entries related to these proteins (Table S7), of which 'genetic disorder' and 'neoplasm' had all association scores above 0.1.

In summary, the bioinformatic analysis suggests that the interaction of GM-CSF with S100A4/A6/P proteins may be relevant to progression of cancer and other disorders. Given that S100A4/A6 antagonizes GM-CSF signalling (Figures 4 and 5), the elevated S100A4/A6/P levels observed in many cancers [75–77] may interfere with anti- and pro-tumorigenic effects of GM-CSF (reviewed in [9]).

4. Conclusions

Examination of the 18 members of S100 protein family for their affinity to GM-CSF shows that in addition to S100A6 [26] and S100P proteins [27], another promiscuous S100 protein [67,68], S100A4, binds GM-CSF *in vitro* with very similar K_d values laying in the micromolar region (Table 1) and resembling those reported for S100A4 interaction with GST-RAGE fusion [62]. Importantly, the lowest estimate of the K_d value is close to the serum S100A4 levels observed in some pathological conditions [71], suggesting a potential (patho)physiological role for the S100A4 – GM-CSF interaction. This conclusion is supported by the effective suppression of the GM-CSF/S100A4-induced changes in viability of THP-1 cells by the extracellular S100A4 (Figure 4).

The S100A4 binding to GM-CSF requires Ca^{2+} binding to S100A4 and its multimerization. Whereas S100A6 binding to GM-CSF follows the same regularities, S100P monomerization causes only a slight decrease in its affinity for GM-CSF (Table 1). Meanwhile, the response of S100A4/A6/P proteins to their monomerization contrasts with that observed for S100P interactions with IL-11 and IFN-β [43,47,66], in which S100P monomerization increases its affinity for the four-helical cytokines by 1.4-2.2 orders of magnitude. These facts demonstrate that the difference in the affinities of dimeric and monomeric forms of a S100 protein to a four-helical cytokine largely depends on the specific cytokine.

The molecular docking data evidence presence of a conserved S100A4/A6/P-binding site in GM-CSF molecule, which overlaps with the residues known to recognize GM-CSF receptors (Figure 3D). These predictions are consistent with the inhibitory effect of extracellular S100A4/A6 proteins on the GM-CSF-induced suppression of viability of THP-1 cells (Figures 4 and 5). The predicted contact residues of S100A4/A6/P dimers are less conserved (Figure 3E). Nevertheless, the predicted involvement of the 'hinge' region and residue F89 of S100P protein in GM-CSF binding was verified by mutagenesis.

Although both GM-CSF and S100A4/A6 suppress viability of THP-1 cells, their combined action inhibits their individual effects (Figures 4 and 5) in accord with the modeling results, similarly to the effects described for S100A1/A4/B/P – IFN-β interactions (MCF-7 cells [42–44]), and for S100A12/A13 binding to soluble TNF (Huh-7 cells [40]). Since S100A6 and S100P interact with 71-73% of the four-helical cytokines studied to date [26,27], the S100 proteins may act as poorly selective inhibitors of their activity. At the same time, S100 binding was shown to promote cytokine signaling in some cases, including activation of the amphiregulin-induced proliferation of fibroblasts by S100A4 [34], and FGF2-medited stimulation of FGFR1 in myoblasts by S100B [39,78]. For this reason, larger-scale studies are needed to establish the functional consequences of the S100-cytokine interactions. Meanwhile, the revealed ability of S100A4/A6/P proteins to interact with GM-CSF and limit its functional activity (S100A4/A6) should be taken into consideration in the clinical use of recombinant GM-CSF and design of the drugs targeting GM-SCF or its receptors.

Supplementary Materials: The following supporting information can be downloaded at: www.mdpi.com/xxx/s1: Figure S1: SPR spectroscopy data on kinetics of association/dissociation of the

complexes of S100P F89A with GM-CSF immobilized on the sensor surface by amine coupling under calcium excess (1 mM CaCl$_2$) at 25°C; Table S1: List of the human diseases associated with GM-CSF and S100A4 protein, according to DisGeNET database; Table S2: List of the human diseases associated with GM-CSF and S100A4 protein, according to OTP database, and corresponding association scores; Table S3: List of the human diseases associated with GM-CSF and S100A6 protein, according to DisGeNET database; Table S4: List of the human diseases associated with GM-CSF and S100A6 protein, according to OTP database, and corresponding association scores; Table S5: List of the human diseases associated with GM-CSF and S100P protein, according to DisGeNET database; Table S6: List of the human diseases associated with GM-CSF and S100P protein, according to OTP database, and corresponding association scores; Table S7: List of the human diseases associated with GM-CSF, S100A4, S100A6 and S100P, according to OTP database, and corresponding association scores.

Author Contributions: Conceptualization, S.E.P.; validation, A.S.K., V.A.R., A.A.V., M.Y.Z., L.A.B., E.I.D., M.P.S., V.N.U., E.A.P., S.E.P.; formal analysis, A.S.K., V.A.R., A.A.V., M.Y.Z., L.A.B., E.I.D., M.P.S., S.E.P.; investigation, A.S.K., V.A.R., A.A.V., M.Y.Z., L.A.B., E.I.D., M.E.P., A.S.S., E.A.L., M.P.S.; data curation, A.S.K., V.A.R., A.A.V., M.Y.Z., L.A.B., E.I.D., M.P.S., S.E.P.; writing—original draft preparation, A.S.K., V.A.R., A.A.V., M.Y.Z., E.I.D., M.E.P., A.S.S., E.A.P., S.E.P.; writing—review and editing, V.A.R., V.N.U., E.A.P., S.E.P.; supervision, E.A.P., S.E.P.; project administration, S.E.P.; funding acquisition, S.E.P. All authors have read and agreed to the published version of the manuscript.

Institutional Review Board Statement: Not applicable.

Informed Consent Statement: Not applicable.

Data Availability Statement: The data present in the current study are available from the corresponding authors on reasonable request.

Conflicts of Interest: The authors declare no conflict of interest. The funders had no role in the design of the study; in the collection, analyses, or interpretation of data; in the writing of the manuscript; or in the decision to publish the results.

Abbreviations

2-ME: 2-mercaptoethanol; AKT, protein kinase B; CCL, C-C motif chemokine ligand; COVID-19, Coronavirus disease 2019; DMSO, dimethyl sulfoxide; DTT, 1,4-dithiothreitol; EDTA, ethylenediaminetetraacetic acid; ELISA, enzyme-linked immunosorbent assay; ERK, extracellular-signal-regulated kinase; FGF, fibroblast growth factor; G-CSF, granulocyte colony-stimulating factor; GM-CSF, granulocyte-macrophage colony-stimulating factor; GST, Glutathione S-transferase; HEPES, 4-(2-hydroxyethyl)piperazine-1-ethanesulfonic acid; IFN, interferon; IL, interleukin; IPTG, isopropyl-β-d-thiogalactoside; IRF, Interferon regulatory factor; JAK, Janus kinase; JMJD3, Jumonji domain-containing protein D3; LPS, lipopolysaccharide; M-CSF, macrophage colony-stimulating factor 1; MEK, Mitogen-activated protein kinase/ERK kinase; mTOR, mammalian target of rapamycin; MTT, 3-(4,5-dimethyl-2-thiazolyl)-2,5-diphenyl-2H-tetrazolium bromide; MWCO, molecular weight cutoff; NF-κB, Nuclear factor kappa-light-chain-enhancer of activated B cells; OTP, Open Targets Platform [61]; PAGE, polyacrylamide gel electrophoresis; PBS, phosphate-buffered saline; PDB, Protein Data Bank [58]; PI3K, phosphoinositide 3-kinase; PMSF, phenylmethylsulfonyl fluoride; RAGE, receptor for advanced glycation end products; RU, resonance unit; SCOP, Structural Classification of Proteins [1]; SDS, sodium dodecyl sulfate; SPR, surface plasmon resonance; STAT, Signal Transducer and Activator of Transcription; TLR, Toll-like receptor; TNF, Tumor necrosis factor; Δ42–47, human S100P mutant lacking PGFLQS sequence in the 'hinge' region, prepared according to [47].

References

1. Andreeva, A.; Kulesha, E.; Gough, J.; Murzin, A.G. The SCOP database in 2020: expanded classification of representative family and superfamily domains of known protein structures. *Nucleic Acids Res* **2020**, *48*, D376-D382, doi:10.1093/nar/gkz1064.
2. Hercus, T.R.; Kan, W.L.T.; Broughton, S.E.; Tvorogov, D.; Ramshaw, H.S.; Sandow, J.J.; Nero, T.L.; Dhagat, U.; Thompson, E.J.; Shing, K., et al. Role of the beta Common (betac) Family of Cytokines in Health and Disease. *Cold Spring Harb Perspect Biol* **2018**, *10*, doi:10.1101/cshperspect.a028514.

3.   Pant, H.; Hercus, T.R.; Tumes, D.J.; Yip, K.H.; Parker, M.W.; Owczarek, C.M.; Lopez, A.F.; Huston, D.P. Translating the biology of β common receptor-engaging cytokines into clinical medicine. *J Allergy Clin Immunol* **2023**, *151*, 324-344, doi:10.1016/j.jaci.2022.09.030.

4.   Dougan, M.; Dranoff, G.; Dougan, S.K. GM-CSF, IL-3, and IL-5 Family of Cytokines: Regulators of Inflammation. *Immunity* **2019**, *50*, 796-811, doi:10.1016/j.immuni.2019.03.022.

5.   Becher, B.; Tugues, S.; Greter, M. GM-CSF: From Growth Factor to Central Mediator of Tissue Inflammation. *Immunity* **2016**, *45*, 963-973, doi:10.1016/j.immuni.2016.10.026.

6.   Conti, L.; Gessani, S. GM-CSF in the generation of dendritic cells from human blood monocyte precursors: recent advances. *Immunobiology* **2008**, *213*, 859-870, doi:10.1016/j.imbio.2008.07.017.

7.   Karlsson, M.; Zhang, C.; Méar, L.; Zhong, W.; Digre, A.; Katona, B.; Sjöstedt, E.; Butler, L.; Odeberg, J.; Dusart, P., et al. A single-cell type transcriptomics map of human tissues. *Sci Adv* **2021**, *7*, doi:10.1126/sciadv.abh2169.

8.   Hamilton, J.A. GM-CSF in inflammation. *J Exp Med* **2020**, *217*, doi:10.1084/jem.20190945.

9.   Kumar, A.; Taghi Khani, A.; Sanchez Ortiz, A.; Swaminathan, S. GM-CSF: A Double-Edged Sword in Cancer Immunotherapy. *Front Immunol* **2022**, *13*, 901277, doi:10.3389/fimmu.2022.901277.

10. Gasson, J.C. Molecular physiology of granulocyte-macrophage colony-stimulating factor. *Blood* **1991**, *77*, 1131-1145, doi:10.1182/blood.v77.6.1131.1131.

11. Francisco-Cruz, A.; Aguilar-Santelises, M.; Ramos-Espinosa, O.; Mata-Espinosa, D.; Marquina-Castillo, B.; Barrios-Payan, J.; Hernandez-Pando, R. Granulocyte-macrophage colony-stimulating factor: not just another haematopoietic growth factor. *Med Oncol* **2014**, *31*, 774, doi:10.1007/s12032-013-0774-6.

12. Bhattacharya, P.; Thiruppathi, M.; Elshabrawy, H.A.; Alharshawi, K.; Kumar, P.; Prabhakar, B.S. GM-CSF: An immune modulatory cytokine that can suppress autoimmunity. *Cytokine* **2015**, *75*, 261-271, doi:10.1016/j.cyto.2015.05.030.

13. Gordon, M.S.; Gabrilove, J.L. Colony-stimulating factors. *Curr Opin Oncol* **1990**, *2*, 1152-1158, doi:10.1097/00001622-199012000-00021.

14. Wu, Y.; Yang, B. Erythropoietin Receptor/beta Common Receptor: A Shining Light on Acute Kidney Injury Induced by Ischemia-Reperfusion. *Frontiers in immunology* **2021**, *12*, 697796, doi:10.3389/fimmu.2021.697796.

15. Lee, K.M.C.; Achuthan, A.A.; Hamilton, J.A. GM-CSF: A Promising Target in Inflammation and Autoimmunity. *Immunotargets Ther* **2020**, *9*, 225-240, doi:10.2147/ITT.S262566.

16. Brown, A.L.; Salerno, D.G.; Sadras, T.; Engler, G.A.; Kok, C.H.; Wilkinson, C.R.; Samaraweera, S.E.; Sadlon, T.J.; Perugini, M.; Lewis, I.D., et al. The GM-CSF receptor utilizes beta-catenin and Tcf4 to specify macrophage lineage differentiation. *Differentiation* **2012**, *83*, 47-59, doi:10.1016/j.diff.2011.08.003.

17. Ribechini, E.; Hutchinson, J.A.; Hergovits, S.; Heuer, M.; Lucas, J.; Schleicher, U.; Jordan Garrote, A.L.; Potter, S.J.; Riquelme, P.; Brackmann, H., et al. Novel GM-CSF signals via IFN-gammaR/IRF-1 and AKT/mTOR license monocytes for suppressor function. *Blood Adv* **2017**, *1*, 947-960, doi:10.1182/bloodadvances.2017006858.

18. Modrowski, D.; Basle, M.; Lomri, A.; Marie, P.J. Syndecan-2 is involved in the mitogenic activity and signaling of granulocyte-macrophage colony-stimulating factor in osteoblasts. *J Biol Chem* **2000**, *275*, 9178-9185, doi:10.1074/jbc.275.13.9178.

19. Sebollela, A.; Cagliari, T.C.; Limaverde, G.S.; Chapeaurouge, A.; Sorgine, M.H.; Coelho-Sampaio, T.; Ramos, C.H.; Ferreira, S.T. Heparin-binding sites in granulocyte-macrophage colony-stimulating factor. Localization and regulation by histidine ionization. *J Biol Chem* **2005**, *280*, 31949-31956, doi:10.1074/jbc.M505314200.

20. Shiomi, A.; Usui, T. Pivotal roles of GM-CSF in autoimmunity and inflammation. *Mediators Inflamm* **2015**, *2015*, 568543, doi:10.1155/2015/568543.

21. Bhattacharya, P.; Budnick, I.; Singh, M.; Thiruppathi, M.; Alharshawi, K.; Elshabrawy, H.; Holterman, M.J.; Prabhakar, B.S. Dual Role of GM-CSF as a Pro-Inflammatory and a Regulatory Cytokine: Implications for Immune Therapy. *J Interferon Cytokine Res* **2015**, *35*, 585-599, doi:10.1089/jir.2014.0149.

22. Lang, F.M.; Lee, K.M.; Teijaro, J.R.; Becher, B.; Hamilton, J.A. GM-CSF-based treatments in COVID-19: reconciling opposing therapeutic approaches. *Nat Rev Immunol* **2020**, *20*, 507-514, doi:10.1038/s41577-020-0357-7.

23. Bonaventura, A.; Vecchie, A.; Wang, T.S.; Lee, E.; Cremer, P.C.; Carey, B.; Rajendram, P.; Hudock, K.M.; Korbee, L.; Van Tassell, B.W., et al. Targeting GM-CSF in COVID-19 Pneumonia: Rationale and Strategies. *Front Immunol* **2020**, *11*, 1625, doi:10.3389/fimmu.2020.01625.

24. Lotfi, N.; Thome, R.; Rezaei, N.; Zhang, G.X.; Rezaei, A.; Rostami, A.; Esmaeil, N. Roles of GM-CSF in the Pathogenesis of Autoimmune Diseases: An Update. *Front Immunol* **2019**, *10*, 1265, doi:10.3389/fimmu.2019.01265.

25. *Granulocyte Macrophage Colony Stimulating Factor Market – Global Industry Analysis and Forecast (2022-2029)*; 69429; 2022.

26. Kazakov, A.S.; Deryusheva, E.I.; Rastrygina, V.A.; Sokolov, A.S.; Permyakova, M.E.; Litus, E.A.; Uversky, V.N.; Permyakov, E.A.; Permyakov, S.E. Interaction of S100A6 Protein with the Four-Helical Cytokines. *Biomolecules* **2023**, *13*, 1345, doi:10.3390/biom13091345.

27. Kazakov, A.S.; Deryusheva, E.I.; Permyakova, M.E.; Sokolov, A.S.; Rastrygina, V.A.; Uversky, V.N.; Permyakov, E.A.; Permyakov, S.E. Calcium-Bound S100P Protein Is a Promiscuous Binding Partner of the Four-Helical Cytokines. *Int J Mol Sci* **2022**, *23*, 12000, doi:10.3390/ijms231912000.

28. Fritz, G.; Heizmann, C.W. 3D Structures of the Calcium and Zinc Binding S100 Proteins. In *Handbook of Metalloproteins*, 2004; https://doi.org/10.1002/0470028637.met046.

29. Donato, R.; Cannon, B.R.; Sorci, G.; Riuzzi, F.; Hsu, K.; Weber, D.J.; Geczy, C.L. Functions of S100 proteins. *Curr Mol Med* **2013**, *13*, 24-57, doi:10.2174/1566524011307010024.

30. Donato, R.; Cannon, B.R.; Sorci, G.; Riuzzi, F.; Hsu, K.; Weber, D.J.; Geczy, C.L. Functions of S100 Proteins. *Curr Mol Med* **2013**, *13*, 24-57.

31. Sreejit, G.; Flynn, M.C.; Patil, M.; Krishnamurthy, P.; Murphy, A.J.; Nagareddy, P.R. S100 family proteins in inflammation and beyond. *Adv Clin Chem* **2020**, *98*, 173-231, doi:10.1016/bs.acc.2020.02.006.

32. Singh, P.; Ali, S.A. Multifunctional Role of S100 Protein Family in the Immune System: An Update. *Cells* **2022**, *11*, doi:10.3390/cells11152274.

33. Holzinger, D.; Foell, D.; Kessel, C. The role of S100 proteins in the pathogenesis and monitoring of autoinflammatory diseases. *Mol Cell Pediatr* **2018**, *5*, 7, doi:10.1186/s40348-018-0085-2.

34. Klingelhofer, J.; Moller, H.D.; Sumer, E.U.; Berg, C.H.; Poulsen, M.; Kiryushko, D.; Soroka, V.; Ambartsumian, N.; Grigorian, M.; Lukanidin, E.M. Epidermal growth factor receptor ligands as new extracellular targets for the metastasis-promoting S100A4 protein. *Febs J* **2009**, *276*, 5936-5948, doi:10.1111/j.1742-4658.2009.07274.x.

35. Pankratova, S.; Klingelhofer, J.; Dmytriyeva, O.; Owczarek, S.; Renziehausen, A.; Syed, N.; Porter, A.E.; Dexter, D.T.; Kiryushko, D. The S100A4 Protein Signals through the ErbB4 Receptor to Promote Neuronal Survival. *Theranostics* **2018**, *8*, 3977-3990, doi:10.7150/thno.22274.

36. Mohan, S.K.; Yu, C. The IL1alpha-S100A13 heterotetrameric complex structure: a component in the non-classical pathway for interleukin 1alpha secretion. *The Journal of biological chemistry* **2011**, *286*, 14608-14617, doi:10.1074/jbc.M110.201954.

37. Carreira, C.M.; LaVallee, T.M.; Tarantini, F.; Jackson, A.; Lathrop, J.T.; Hampton, B.; Burgess, W.H.; Maciag, T. S100A13 is involved in the regulation of fibroblast growth factor-1 and p40 synaptotagmin-1 release in vitro. *Journal of Biological Chemistry* **1998**, *273*, 22224-22231, doi:10.1074/jbc.273.35.22224.

38. Gupta, A.A.; Chou, R.H.; Li, H.C.; Yang, L.W.; Yu, C. Structural insights into the interaction of human S100B and basic fibroblast growth factor (FGF2): Effects on FGFR1 receptor signaling. *Bba-Proteins Proteom* **2013**, *1834*, 2606-2619, doi:10.1016/j.bbapap.2013.09.012.

39. Riuzzi, F.; Sorci, G.; Donato, R. S100B protein regulates myoblast proliferation and differentiation by activating FGFR1 in a bFGF-dependent manner. *J Cell Sci* **2011**, *124*, 2389-2400, doi:10.1242/jcs.084491.

40. Kazakov, A.S.; Zemskova, M.Y.; Rystsov, G.K.; Vologzhannikova, A.A.; Deryusheva, E.I.; Rastrygina, V.A.; Sokolov, A.S.; Permyakova, M.E.; Litus, E.A.; Uversky, V.N., et al. Specific S100 Proteins Bind Tumor Necrosis Factor and Inhibit Its Activity. *Int J Mol Sci* **2022**, *23*, 15956, doi:10.3390/ijms232415956.

41. Kazakov, A.S.; Deryusheva, E.I.; Sokolov, A.S.; Permyakova, M.E.; Litus, E.A.; Rastrygina, V.A.; Uversky, V.N.; Permyakov, E.A.; Permyakov, S.E. Erythropoietin Interacts with Specific S100 Proteins. *Biomolecules* **2022**, *12*, 120, doi:10.3390/biom12010120.

42. Kazakov, A.S.; Sofin, A.D.; Avkhacheva, N.V.; Denesyuk, A.I.; Deryusheva, E.I.; Rastrygina, V.A.; Sokolov, A.S.; Permyakova, M.E.; Litus, E.A.; Uversky, V.N., et al. Interferon Beta Activity Is Modulated via Binding of Specific S100 Proteins. *International journal of molecular sciences* **2020**, *21*, 9473, doi:10.3390/ijms21249473.

43. Kazakov, A.S.; Mayorov, S.A.; Deryusheva, E.I.; Avkhacheva, N.V.; Denessiouk, K.A.; Denesyuk, A.I.; Rastrygina, V.A.; Permyakov, E.A.; Permyakov, S.E. Highly specific interaction of monomeric S100P protein with interferon beta. *Int J Biol Macromol* **2020**, *143*, 633-639, doi:10.1016/j.ijbiomac.2019.12.039.

44. Kazakov, A.S.; Sofin, A.D.; Avkhacheva, N.V.; Deryusheva, E.I.; Rastrygina, V.A.; Permyakova, M.E.; Uversky, V.N.; Permyakov, E.A.; Permyakov, S.E. Interferon-β Activity Is Affected by S100B Protein. *International journal of molecular sciences* **2022**, *23*, 1997, doi:10.3390/ijms23041997.

45. Kazakov, A.S.; Sokolov, A.S.; Permyakova, M.E.; Litus, E.A.; Uversky, V.N.; Permyakov, E.A.; Permyakov, S.E. Specific cytokines of interleukin-6 family interact with S100 proteins. *Cell Calcium* **2022**, *101*, 102520, doi:10.1016/j.ceca.2021.102520.

46. Kazakov, A.S.; Sokolov, A.S.; Vologzhannikova, A.A.; Permyakova, M.E.; Khorn, P.A.; Ismailov, R.G.; Denessiouk, K.A.; Denesyuk, A.I.; Rastrygina, V.A.; Baksheeva, V.E., et al. Interleukin-11 binds specific EF-hand proteins via their conserved structural motifs. *J Biomol Struct Dyn* **2017**, *35*, 78-91, doi:10.1080/07391102.2015.1132392.

47. Kazakov, A.S.; Sokolov, A.S.; Rastrygina, V.A.; Solovyev, V.V.; Ismailov, R.G.; Mikhailov, R.V.; Ulitin, A.B.; Yakovenko, A.R.; Mirzabekov, T.A.; Permyakov, E.A., et al. High-affinity interaction between interleukin-11 and S100P protein. *Biochem Biophys Res Commun* **2015**, *468*, 733-738, doi:10.1016/j.bbrc.2015.11.024.

48. Bresnick, A.R. S100 proteins as therapeutic targets. *Biophys Rev* **2018**, *10*, 1617-1629, doi:10.1007/s12551-018-0471-y.

49. Zhou, Y.; Zha, Y.; Yang, Y.; Ma, T.; Li, H.; Liang, J. S100 proteins in cardiovascular diseases. *Mol Med* **2023**, *29*, 68, doi:10.1186/s10020-023-00662-1.

50. Goswami, D.; Anuradha, U.; Angati, A.; Kumari, N.; Singh, R.K. Pharmacological and Pathological Relevance of S100 Proteins in Neurological Disorders. *CNS Neurol Disord Drug Targets* **2023**, *22*, 1403-1416, doi:10.2174/1871527322666221128160653.

51. Hao, W.; Zhang, Y.; Dou, J.; Cui, P.; Zhu, J. S100P as a potential biomarker for immunosuppressive microenvironment in pancreatic cancer: a bioinformatics analysis and in vitro study. *BMC Cancer* **2023**, *23*, 997, doi:10.1186/s12885-023-11490-1.

52. Pace, C.N.; Vajdos, F.; Fee, L.; Grimsley, G.; Gray, T. How to measure and predict the molar absorption coefficient of a protein. *Protein Sci.* **1995**, *4*, 2411-2423, doi:10.1002/pro.5560041120

53. LaVallie, E.R.; DiBlasio, E.A.; Kovacic, S.; Grant, K.L.; Schendel, P.F.; McCoy, J.M. A thioredoxin gene fusion expression system that circumvents inclusion body formation in the E. coli cytoplasm. *Biotechnology (N Y)* **1993**, *11(2)*, 187-193, doi:10.1038/nbt0293-187.

54. Sokolov, A.S.; Kazakov, A.S.; Solovyev, V.V.; Ismailov, R.G.; Uversky, V.N.; Lapteva, Y.S.; Mikhailov, R.V.; Pavlova, E.V.; Terletskaya, I.O.; Ermolina, L.V., et al. Expression, Purification, and Characterization of Interleukin-11 Orthologues. *Molecules* **2016**, *21*, doi:10.3390/molecules21121632.

55. Catanzariti, A.M.; Soboleva, T.A.; Jans, D.A.; Board, P.G.; Baker, R.T. An efficient system for high-level expression and easy purification of authentic recombinant proteins. *Protein Sci* **2004**, *13*, 1331-1339, doi:10.1110/ps.04618904.

56. Burstein, E.A.; Emelyanenko, V.I. Log-normal description of fluorescence spectra of organic fluorophores. *Photocem.Photobiol.* **1996**, *64*, 316-320.

57. Desta, I.T.; Porter, K.A.; Xia, B.; Kozakov, D.; Vajda, S. Performance and Its Limits in Rigid Body Protein-Protein Docking. *Structure* **2020**, *28*, 1071-1081 e1073, doi:10.1016/j.str.2020.06.006.

58. Berman, H.M.; Westbrook, J.; Feng, Z.; Gilliland, G.; Bhat, T.N.; Weissig, H.; Shindyalov, I.N.; Bourne, P.E. The Protein Data Bank. *Nucleic Acids Res.* **2000**, *28*, 235-242.

59. Schrodinger, LLC. The PyMOL Molecular Graphics System, Version 1.8. 2015.

60. Pinero, J.; Ramirez-Anguita, J.M.; Sauch-Pitarch, J.; Ronzano, F.; Centeno, E.; Sanz, F.; Furlong, L.I. The DisGeNET knowledge platform for disease genomics: 2019 update. *Nucleic Acids Res* **2020**, *48*, D845-D855, doi:10.1093/nar/gkz1021.

61. Carvalho-Silva, D.; Pierleoni, A.; Pignatelli, M.; Ong, C.; Fumis, L.; Karamanis, N.; Carmona, M.; Faulconbridge, A.; Hercules, A.; McAuley, E., et al. Open Targets Platform: new developments and updates two years on. *Nucleic Acids Res* **2019**, *47*, D1056-D1065, doi:10.1093/nar/gky1133.

62. Leclerc, E.; Fritz, G.; Vetter, S.W.; Heizmann, C.W. Binding of S100 proteins to RAGE: an update. *Biochim Biophys Acta* **2009**, *1793*, 993-1007, doi:10.1016/j.bbamcr.2008.11.016.

63. Lv, Y.; Niu, Z.; Guo, X.; Yuan, F.; Liu, Y. Serum S100 calcium binding protein A4 (S100A4, metatasin) as a diagnostic and prognostic biomarker in epithelial ovarian cancer. *Br J Biomed Sci* **2018**, *75*, 88-91, doi:10.1080/09674845.2017.1394052.

64. Pathuri, P.; Vogeley, L.; Luecke, H. Crystal structure of metastasis-associated protein S100A4 in the active calcium-bound form. *J Mol Biol* **2008**, *383*, 62-77, doi:10.1016/j.jmb.2008.04.076.

65. Malashkevich, V.N.; Varney, K.M.; Garrett, S.C.; Wilder, P.T.; Knight, D.; Charpentier, T.H.; Ramagopal, U.A.; Almo, S.C.; Weber, D.J.; Bresnick, A.R. Structure of Ca2+-bound S100A4 and its interaction with peptides derived from nonmuscle myosin-IIA. *Biochemistry* **2008**, *47*, 5111-5126, doi:10.1021/bi702537s.

66. Permyakov, S.E.; Denesyuk, A.I.; Denessiouk, K.A.; Permyakova, M.E.; Kazakov, A.S.; Ismailov, R.G.; Rastrygina, V.A.; Sokolov, A.S.; Permyakov, E.A. Monomeric state of S100P protein: Experimental and molecular dynamics study. *Cell Calcium* **2019**, *80*, 152-159, doi:10.1016/j.ceca.2019.04.008.

67. Simon, M.A.; Ecsedi, P.; Kovacs, G.M.; Poti, A.L.; Remenyi, A.; Kardos, J.; Gogl, G.; Nyitray, L. High-throughput competitive fluorescence polarization assay reveals functional redundancy in the S100 protein family. *The FEBS journal* **2020**, *287*, 2834-2846, doi:10.1111/febs.15175.

68. Simon, M.A.; Bartus, É.; Mag, B.; Boros, E.; Roszjár, L.; Gógl, G.; Travé, G.; Martinek, T.A.; Nyitray, L. Promiscuity mapping of the S100 protein family using a high-throughput holdup assay. *Sci Rep* **2022**, *12*, 5904, doi:10.1038/s41598-022-09574-2.

69. Madeira, F.; Park, Y.M.; Lee, J.; Buso, N.; Gur, T.; Madhusoodanan, N.; Basutkar, P.; Tivey, A.R.N.; Potter, S.C.; Finn, R.D., et al. The EMBL-EBI search and sequence analysis tools APIs in 2019. *Nucleic Acids Res* **2019**, *47*, W636-W641, doi:10.1093/nar/gkz268.

70. Del Toro, N.; Shrivastava, A.; Ragueneau, E.; Meldal, B.; Combe, C.; Barrera, E.; Perfetto, L.; How, K.; Ratan, P.; Shirodkar, G., et al. The IntAct database: efficient access to fine-grained molecular interaction data. *Nucleic Acids Res* **2022**, *50*, D648-D653, doi:10.1093/nar/gkab1006.

71. Oughtred, R.; Rust, J.; Chang, C.; Breitkreutz, B.J.; Stark, C.; Willems, A.; Boucher, L.; Leung, G.; Kolas, N.; Zhang, F., et al. The BioGRID database: A comprehensive biomedical resource of curated protein, genetic,

and chemical interactions. *Protein science : a publication of the Protein Society* **2021**, *30*, 187-200, doi:10.1002/pro.3978.

72. Chanput, W.; Mes, J.J.; Wichers, H.J. THP-1 cell line: an in vitro cell model for immune modulation approach. *Int Immunopharmacol* **2014**, *23*, 37-45, doi:10.1016/j.intimp.2014.08.002.

73. Fujita, Y.; Matsuoka, N.; Temmoku, J.; Furuya-Yashiro, M.; Asano, T.; Sato, S.; Matsumoto, H.; Watanabe, H.; Kozuru, H.; Yatsuhashi, H., et al. JAK inhibitors impair GM-CSF-mediated signaling in innate immune cells. *BMC Immunol* **2020**, *21*, 35, doi:10.1186/s12865-020-00365-w.

74. Schwarz, H.; Schmittner, M.; Duschl, A.; Horejs-Hoeck, J. Residual endotoxin contaminations in recombinant proteins are sufficient to activate human CD1c+ dendritic cells. *PLoS One* **2014**, *9*, e113840, doi:10.1371/journal.pone.0113840.

75. Bresnick, A.R.; Weber, D.J.; Zimmer, D.B. S100 proteins in cancer. *Nat Rev Cancer* **2015**, *15*, 96-109, doi:10.1038/nrc3893.

76. Hua, X.; Zhang, H.M.; Jia, J.F.; Chen, S.S.; Sun, Y.; Zhu, X.L. Roles of S100 family members in drug resistance in tumors: Status and prospects. *Biomed Pharmacother* **2020**, *127*, doi:10.1016/J.Biopha.2020.110156.

77. Chen, H.; Xu, C.; Jin, Q.; Liu, Z. S100 protein family in human cancer. *Am J Cancer Res* **2014**, *4*, 89-115.

78. Riuzzi, F.; Sorci, G.; Beccafico, S.; Donato, R. S100B engages RAGE or bFGF/FGFR1 in myoblasts depending on its own concentration and myoblast density. Implications for muscle regeneration. *PLoS One* **2012**, *7*, e28700, doi:10.1371/journal.pone.0028700.